

FEDSM-ICNMM2010-30* \$%

FIBER TRANSPORT AND DEPOSITION IN HUMAN UPPER TRACHEOBRONCHIAL AIRWAYS

L. Tian

Department of Science & Engineering
Technology, SUNY Canton
Canton, NY, USA
tianl@canton.edu

G. Ahmadi

Department of Aeronautical and
Mechanical Engineering, Clarkson University
Potsdam, NY, USA
ahmadi@clarkson.edu

P. K. Hopke

Department of Chemical Engineering
Clarkson University
Potsdam, NY, USA
hopkepk@clarkson.edu

Y-S. Cheng

Lovelace Respiratory Research Institute
Albuquerque, NM, USA
ycheng@lrri.org

ABSTRACT

Transport and deposition of inhaled asbestos fibers has been studied in the past few decades due to its pathological response in living being. Of the earlier study, in vitro and vivo experiments in human and animal subjects were conducted and measurements were made where carcinogenicity of these particles was investigated. In this work, the transport and deposition of elongated ellipsoidal fibers were numerically simulated in a physiological realistic multi-level lung model. Detailed motion of the inhaled fibers and their interaction with the surrounding environment were reproduced by solving the system of coupled nonlinear equations governing the fibers' translational and rotational motion. This information has never been revealed in past studies. Correlations between the deposition pattern, fiber characteristics, breathing conditions, and airway morphology in human upper tracheobronchial airways were analyzed. The results were compared with experimental measurements, and carcinogenicity of these fibers was discussed.

Keywords: Asbestos, elongated mineral particles (EMP), fiber, transport, deposition, tracheobronchial tree, numerical simulation, airway bifurcation model, turbulence.

INTRODUCTION

Occupational exposure to asbestos fibers or elongated mineral particles (EMPs) has been linked to the occurrence of malignant respiratory diseases such as mesothelioma and lung cancer. Widely accepted, the respiratory pathological response in living being is mainly induced by the retention and deposition of the inhaled asbestos fibers. Measurements of such deposition in human patient tissues as well as in vivo animal studies were reported by many researchers, such as Lippmann et al. (1988, 1990), Berman et al. (1995), and Suzuki et al. (2005). Based on the available data EPA (2003) concluded that fibers with length shorter than 5 μm posed minimum risk, while the threshold for diameter needed further investigation. NIOSH (2008) concluded that fibers with length smaller than 1.5 μm or greater than 40 μm and diameter thinner than 0.25 μm or thicker than 3 μm , respectively, were at the highest risk to cause lung cancer.

The lack of theoretical and numerical study of asbestos fibers in airway passages was mainly due to its complexity. The fibers' translational and rotational motion was governed by system of coupled nonlinear equations which posed enormous challenge for direct solution in 3D airway passages. Among the few fundamental studies, Jeffery (1922) evaluated the drag

and torque acting on an elongated ellipsoidal fiber in a creeping flow, and the rotational motion in a simple shear was derived. Most of the earlier theoretical and numerical studies were based on simplified flow field where either analytical solution was available or shear of the flow was assumed constant.

In this study, simulation of the transport and deposition of elongated ellipsoidal fibers in a physiologically realistic human airway model was conducted. Mathematical description of fiber motion was given by system of coupled nonlinear equations accounting for the hydrodynamic drag and torque, shear induced lift, Brownian diffusion, and the gravitational sedimentation. The simulated results provided detailed information for analyzing the contribution of fiber dimensional characteristics (length, diameter, aspect ratio, density) toward deposition. Effect of the airflow pattern and airway morphology was also derived. Results of the study were compared to earlier experimental measurements, and carcinogenicity of the fiber in relation to its dimensional characteristics was discussed.

HUMAN TRACHEOBRONCHIAL TREE

Multi-Level Computational Model of Lung

Originated from Weibel's (1963) idea that the human tracheobronchial tree was modeled as repeated bifurcations from the trachea (G0, generation 0) to the alveoli (G23, generation 23), in the current study, a multi-level computational model for simulation of airflow and particle transport in the lung is proposed. In this approach, a single lung bifurcation (Figure 1) serves as the base model element, and the subsequent airway generations are generated by scaling down the base element according to the airway specifications (as suggested by Weibel (1963)). The entire tracheobronchial tree (with the exception of the alveolar region) can be constructed by fusing a sequence of these base elements. The schematic of the multi-level bifurcation model of human tracheobronchial upper airways (G0 to G3) is shown in Figure 2.

FIBER MODEL

Figure 3 shows a sample elongated fiber particle. The relationship between elongated particle transport and deposition and its geometric characteristic are numerically analyzed in this study. Details of the fiber transport model in an arbitrary flow can be found in the work of Fan and Ahmadi (1995).

AIRFLOW SIMULATION

Laminar flow is assumed in lower level tracheobronchial airways where the mass continuity and Navier-Stokes equations are governing the flow

motion. At trachea and the first two airway generations, Reynolds stress turbulence model is used to describe the flow motion, Tian and Ahmadi (2007).

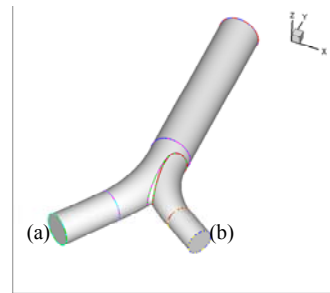


Figure 1. Asymmetric single tracheobronchial bifurcation model.

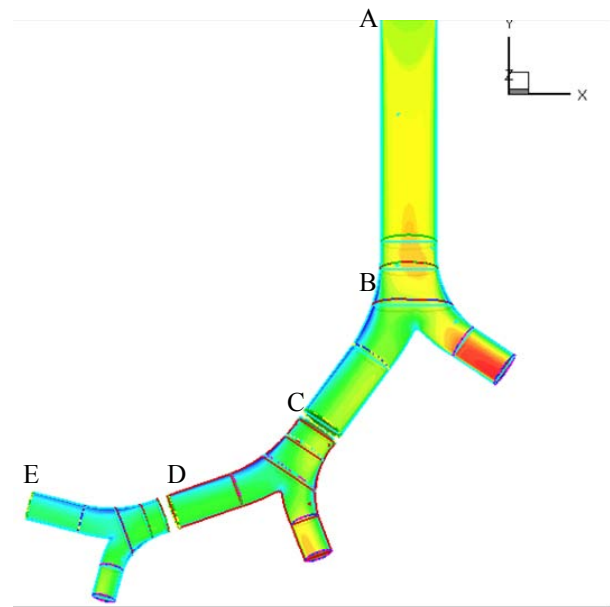


Figure 2. Schematic of the multi-level bifurcation model of human tracheobronchial upper airways (G0 to G3): AB - Trachea, BC - Bifurcation 1, CD - Bifurcation 2, DE - bifurcation 3.

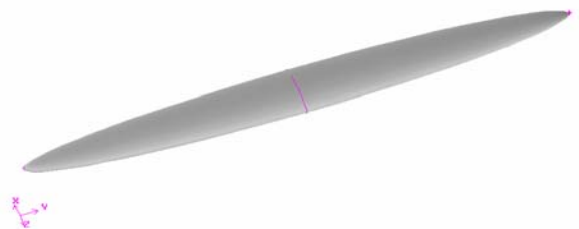


Figure 3. Elongated fiber particle.

FIBER EQUATION OF MOTION

The translational motion of the fibers is governed by Newton's second law:

$$m^p \frac{d\mathbf{v}}{dt} = m^p \mathbf{g} + \mathbf{f}^h + \mathbf{f}^L, \quad (12)$$

The governing equations of rotational motions of the fibers are:

$$I_{\hat{x}} \frac{d\omega_{\hat{x}}}{dt} - \omega_{\hat{y}} \omega_{\hat{z}} (I_{\hat{y}} - I_{\hat{z}}) = T_{\hat{x}}^h, \quad (13)$$

$$I_{\hat{y}} \frac{d\omega_{\hat{y}}}{dt} - \omega_{\hat{z}} \omega_{\hat{x}} (I_{\hat{z}} - I_{\hat{x}}) = T_{\hat{y}}^h, \quad (14)$$

$$I_{\hat{z}} \frac{d\omega_{\hat{z}}}{dt} - \omega_{\hat{x}} \omega_{\hat{y}} (I_{\hat{x}} - I_{\hat{y}}) = T_{\hat{z}}^h, \quad (15)$$

Here \mathbf{V} is the velocity vector of the fiber particle mass center in the fixed coordinate, and $(\omega_{\hat{x}}, \omega_{\hat{y}}, \omega_{\hat{z}})$ is the angular velocity vector of the fiber in the particle frame (Cartesian coordinate attached to the fiber centroid with its axes parallel to the fiber's principle axis). m^p is the mass of the fiber, \mathbf{g} is the acceleration of gravity, \mathbf{f}^h is the hydrodynamic force and \mathbf{f}^L is the shear induced lift force. $(I_{\hat{x}}, I_{\hat{y}}, I_{\hat{z}})$ is the moments of inertia of the fiber about the principle axes in the particle frame $(\hat{x}, \hat{y}, \hat{z})$, and $(T_{\hat{x}}^h, T_{\hat{y}}^h, T_{\hat{z}}^h)$ is the hydrodynamic torques acting on the particle with respect to the principle axes in the particle frame.

RESULTS AND DISCUSSION

Figure 4 displays the simulated fiber motion in the human upper tracheobronchial airway. Upon entering the airway generation adjacent to the wall, the fiber tends to align itself with the main flow while traveling to deeper lung. Occasional rotation is observed, however the fiber quickly returns to its alignment position. Figure 4 clearly shows the coupling between its translational and rotational motion. The coupling has profound effect in predicting its position at complex flow domain – the partition at the bifurcation in Figure 4.

Figure 5 displays the simulated fiber deposition pattern in the human upper tracheobronchial airways up to the third bifurcation for fibers with aspect ratio of 15 and 80, diameter of $3.66\mu\text{m}$ and breathing rates of 40L/min and 15L/min at the trachea. It is shown in Figure 5a that the deposition sites of the elongated fibers are highly localized in the trachea and the first bifurcation. It is also seen from Figure 5a that the fiber deposition is significantly enhanced with its aspect ratio from 15 to 80. Figure 5b displays the fiber deposition pattern in the second bifurcation. While the deposition rate is enhanced as the fiber aspect ratio is increased, the deposition is more uniformly distributed across the airway surfaces. Figure 5c displays the fiber deposition pattern in the third bifurcation at the light

breathing condition with 15L/min at the trachea. It is observed that most of the fibers entering the third bifurcation penetrate through. The effect of fiber aspect ratio toward the deposition is less significant.

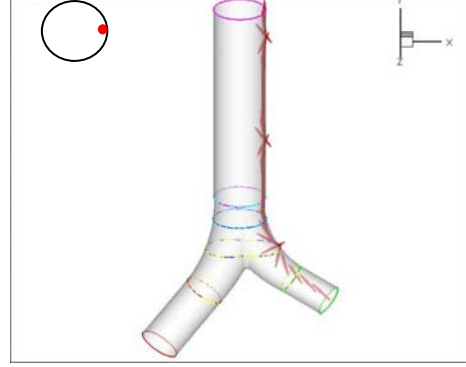


Figure 4. Simulated fiber motion in the upper airway.

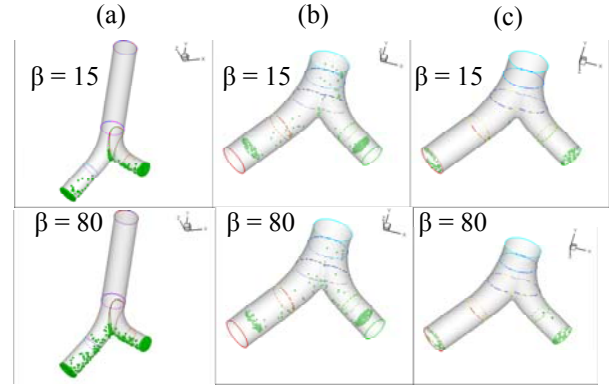


Figure 5. Fiber (diameter = $3.66\mu\text{m}$) deposition pattern in the human upper tracheobronchial airways: (a) Trachea and first bifurcation (40L/min); (b) Second bifurcation (40L/min at the trachea and 20L/min at the inlet of the second bifurcation); (c) Third bifurcation (15L/min at the trachea and 5L/min at the inlet of the third bifurcation).

Figure 6 compares the predicted fiber deposition efficiency in the third bifurcation (Generation 2 and 3). Experimental measurements of Zhou et al. (2007) and Wang and Hopke (2008) are plotted in this figure for comparison. Carbon fibers of diameter $3.66\mu\text{m}$, and aspect ratios from 1 to 80 are used in these simulations. Light to moderate breathing conditions of 15 to 40 L/min are also considered. It is shown that deposition rate increases with the increase of the non-dimensional relaxation time, while the measured data are quite scattered. It is also observed that the stronger the breathing intensity, the higher the deposition rate.

According to Tian and Ahmadi (2007), the near wall correction on the turbulence fluctuation near a surface is essential for correct prediction of the particle deposition rates in turbulent flows. The present

simulation accounts for this correction by using the turbulence near wall “two-layer zonal model” and the “quadratic variation near wall model”. A series of simulations for wall corrections being made assuming a range of u^* are performed and the results are presented in Figure 6. By altering the flow shear velocity for the turbulence near wall correction, the numerical simulation leads to slightly different deposition rates, all of which are in range of the experimental data. This result implies a weak turbulence activity in the third bifurcation. One set of simulation is performed with laminar model in bifurcation 3 at lower breathing rate of 15L/min. The predicted data corresponds well with the experimental measurement, though statistical fluctuations are observed due to very low deposition rate ($< 1\%$).

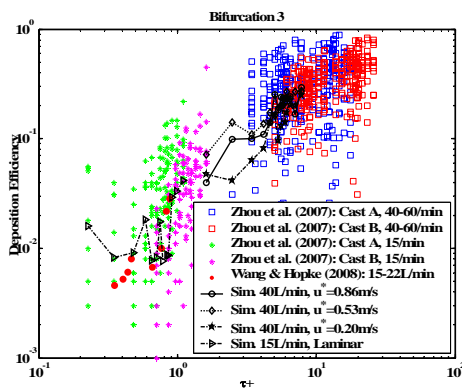


Figure 6. Comparison of the fiber deposition efficiency in the third bifurcation

CONCLUSIONS

This work simulated the transport and deposition of fiber in a physiologically realistic human airway model. The simulated results verified the coupling between the fiber’s translational and rotational motion, and the importance of including the coupling effect for the accurate prediction of fiber motion in human lung. The deposition pattern and deposition rate were calculated based on the simulation results. It was shown that the deposition sites and rate are highly dependent on fiber’s geometric characteristic that is the fiber length and diameter. The result correlates to the findings of EPA (2003) and NIOSH (2008). The computational simulation also finds the close correlation of the fiber deposition rate with the flow pattern. Further research will be focused on quantitative comparisons with the.

ACKNOWLEDGEMENT

This work is supported by National Institute for Occupational Safety and Health (NIOSH) and Center

for Air Resources Engineering and Science at Clarkson University.

REFERENCES

- Berman, D.W., Crump, K.S., Chatfield, E.J., Davis, J.M.G., and Jones, A.D., 1995, “The sizes, shapes, and mineralogy of asbestos structures that induce lung tumors or mesothelioma in AF/HAN rats following inhalation”, *Risk Anal* 15: pp.181–195.
- EPA (U.S. Environmental Protection Agency), 2003, “Report on the Peer Consultation Workshop to Discuss a Proposed Protocol to Assess Asbestos-Related Risk, Final Report”, Office of Solid Waste and Emergency Response, Washington D.C.
- Fan, F.G. and Ahmadi, G., 1995, “A sublayer model for wall deposition of ellipsoidal particles in turbulent streams”, *J. of Aerosol Science*, 26, pp. 831-840.
- Heistracher, H and Hofmann, W., 1995, “Physiologically Realistic Models of Bronchial Airway Bifurcations”, *J. of Aerosol Science*, 26, pp. 497-509.
- Jeffery, G.B., 1922, “The motion of ellipsoidal particles immersed in a viscous fluid”, *Proceedings of the Royal Society A*, 102, pp., 161-179.
- Lippmann, M, 1988, “Asbestos exposure indices”, *Environ Res.*, 46, pp., 86–106.
- Lippmann, M, 1990, “Effects of fiber characteristics on lung deposition, retention, and disease”, *Environ Health Perspect*, 88, pp. 311–317.
- NIOSH, 2005, “Comments on the MSHA Proposed Rule on Asbestos Exposure Limit”.
- Phillips, C.G. and Kaye S.R., 1997, “On the Asymmetry of Bifurcations in the Bronchial Tree”, *Respiration Physiology*, 107, pp. 85-98.
- Suzuki, Y, Yuen, S, and Ashley, R, 2005, “Short thin asbestos fibers contribute to the development of human malignant mesothelioma: pathological evidence”, *Int J Hyg Environ Health* 208, pp. 201–210.
- Tian, L. and Ahmadi, G., 2007, “Particle Deposition in Turbulent Duct Flows – Comparisons of Different Model Predictions”, *J. of Aerosol Science*, 38, pp. 377-397.
- Weibel, E. R., 1963, “Morphometry of the Human Lung”, New York.: Academic Press.
- Zhou, Y., Su, W-C and Cheng, Y.S., 2007, “Fiber Deposition in the Tracheobronchial Region: Experimental Measurements”, *Inhalation Toxicology*, 19, pp. 1071-1078.